Metabolism in Vitro and in Vivo of the DNA Base Adduct, M_1G

Charles G. Knutson,[†] Dapo Akingbade,[†] Brenda C. Crews,[†] Markus Voehler,[‡] Donald F. Stec,[‡] and Lawrence J. Marnett*[,†,‡,§]

A.B. Hancock Jr. Memorial Laboratory for Cancer Research, Departments of Biochemistry, Chemistry, and Pharmacology, Vanderbilt Institute of Chemical Biology, Center in Molecular Toxicology, Vanderbilt-Ingram Cancer Center, Vanderbilt University School of Medicine, Nashville, Tennessee 37232-0146

Received November 22, 2006

Oxidative damage is considered a major contributing factor to genetic diseases including cancer. Our laboratory is evaluating endogenously formed DNA adducts as genomic biomarkers of oxidative injury. Recent efforts have focused on investigating the metabolic stability of adducts in vitro and in vivo. Here, we demonstrate that the base adduct, M_1G, undergoes oxidative metabolism in vitro in rat liver cytosol (RLC, $K_m = 105\ \mu M$ and $v_{max}/K_m = 0.005\ min^{-1}\ mg^{-1}$) and in vivo when administered intravenously to male Sprague Dawley rats. LC-MS analysis revealed two metabolites containing successive additions of 16 amu. One- and two-dimensional NMR experiments showed that oxidation occurred first at the 6-position of the pyrimido ring, forming 6-oxo-M_1G, and then at the 2-position of the imidazole ring, yielding 2,6-dioxo-M_1G. Authentic 6-oxo-M_1G was chemically synthesized and observed to undergo metabolism to 2,6-dioxo-M_1G in RLC ($K_m = 210\ \mu M$ and $v_{max}/K_m = 0.005\ min^{-1}\ mg^{-1}$). Allopurinol partially inhibited M_1G metabolism (75%) and completely inhibited 6-oxo-M_1G metabolism in RLC. These inhibition studies suggest that xanthine oxidase is the principal enzyme acting on M_1G in RLC and the only enzyme that converts 6-oxo-M_1G to 2,6-dioxo-M_1G. Both M_1G and 6-oxo-M_1G are better substrates (5-fold) for oxidative metabolism in RLC than the deoxynucleoside, M_1dG. Alternative repair pathways or biological processing of M_1dG makes the fate of M_1G of interest as a potential marker of oxidative damage in vivo.

Introduction

Oxidative damage is considered a causative step in the progression of many genetic diseases including cancer (*1*). Evaluating genomic exposure to oxidative damage may have an impact in risk assessment (*2*). It has been suggested that monitoring DNA adduct formation is a useful diagnostic tool in human populations (*3*) and is commonly employed by multiple laboratories (*4*−*7*).

The pyrimidopurinone adduct, M_1dG, forms from reactions of 2′-deoxyguanosine (dG) with either the DNA peroxidation product, base propenal (*8*−*10*), or the lipid peroxidation product, malondialdehyde (*10*−*12*) (Scheme 1). M_1dG is mutagenic in bacterial and mammalian cells (*13*−*16*) and can be extracted from the genomic DNA of humans and animals (*17*−*19*). M_1-dG is reported to be a substrate for the nucleotide excision repair pathway (NER), which accounts for its appearance in human urine (*13*, *20*). This repair-dependent removal and subsequent deposition into urine provides an available source of M_1dG for monitoring the exposure to oxidative damage (*21*).

Many endogenously produced exocyclic ring adducts are substrates for base excision repair (BER) (*22*). Some adducts are subject to multiple repair pathways (i.e., 8-oxo-dG is repaired by BER and, presumably, NER machinery (*23*, *24*)). Etheno adducts bearing structural similarity to M_1dG (e.g., 1,N^2-etheno-dG, 1,N^6-etheno-deoxyadenosine, and 3,N^4-etheno-deoxycytidine) are substrates for BER enzymes and DNA glycosylases (*25*−*29*). The structural resemblance between M_1dG and the etheno adducts might suggest that similar, yet unknown, repair pathways are also involved in the repair of M_1dG. Emerging

Scheme 1. Formation of M_1dG from Endogenous Sources and Possible Routes of Release from DNA

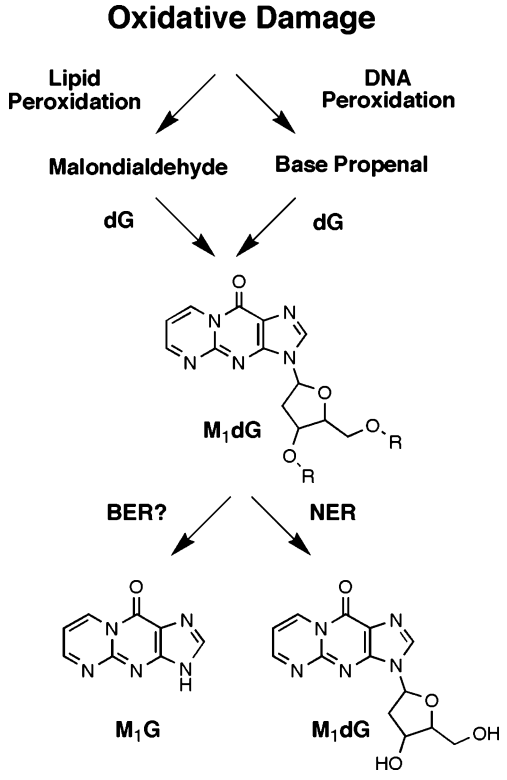

* Corresponding author. Fax: (615) 343-7534. E-mail: larry.marnett@vanderbilt.edu.
† Department of Biochemistry.
‡ Department of Chemistry.
§ Department of Pharmacology.

10.1021/tx600334x CCC: $37.00
Published on Web 02/21/2007

discoveries regarding the induction of BER enzymes in vivo in response to stress has made alternate routes of repair of particular interest (*30*, *31*).

Our laboratory recently demonstrated that M_1dG was oxidized to 6-oxo-M_1dG in rats and that xanthine oxidase (XO) and aldehyde oxidase (AO) were the likely enzymes responsible (*32*). M_1dG oxidation was detected in rat and human liver cytosols and was metabolized in purified bovine XO. In all cases, 6-oxo-M_1dG was the sole product, and there was no evidence for oxidation on the imidazole ring. This was surprising because the imidazole ring is the primary site for chemical oxidation on dG and a site for oxidation on xanthine by XO. The present article describes the in vitro and in vivo oxidation of the base, M_1G, a putative product of repair in M_1dG-containing DNA by glycosylase action. Results from our metabolism studies on M_1G show that it is a better substrate for enzymatic oxidation than M_1dG. Furthermore, its initial oxidation product, 6-oxo-M_1G, is susceptible to further oxidation on the imidazole ring. When administered to Sprague Dawley rats, M_1G and both of the oxidized metabolites were excreted in urine. Thus, a family of oxidized metabolites may serve as biomarkers of M_1dG formation in genomic DNA.

Materials and Methods

All chemicals were obtained from commercial sources and used as received. Solvents were of HPLC grade purity or higher. M_1G was synthesized as previously described (*33*). Rat liver cytosol (RLC) was prepared by established methods (*34*). Purified bovine XO was purchased from CalBiochem (La Jolla, CA). HPLC-UV separations were performed on a Waters 2695 autosampler and binary pump with a Waters 2487 dual wavelength UV detector (Milford, MA). LC-MS/MS spectra were obtained on a ThermoFinnigan LCQ Deca-XP Ion Trap (San Jose, CA) with an inline Agilent 1100 series dual binary pump (Santa Clara, CA). Synthetic chemicals were purified by flash chromatography on a Biotage SP1 Instrument (Uppsala, Sweden).

M_1G Treatment of Rats. Animal protocols were performed under the approval of Vanderbilt University and in accordance with the Institutional Animal Care and Use Committee policies. Male Sprague Dawley rats (225−250 g) with vascular catheters surgically implanted in the femoral and jugular veins were obtained from Charles River Laboratories (Wilmington, MA) and housed in shoebox cages. The animals were transferred to metabolism cages prior to dosing and allowed to feed *ad libitum* throughout the experiment. The M_1G dosing solution (5 mg/kg) was prepared in sterile saline and administered in the jugular catheter in approximately 0.5 mL of total volume over 45 s and flushed with 0.4 mL of sterile heparinized saline. Urine and feces were collected over intervals (pre-dose, 0−4, 4−6, 6−10, and 10−24 h). All samples were stored at −80 °C until sample workup.

Sample Workup and Analysis. A sample of urine (25% of the total collected volume) was extracted by adding 2× volumes of ethanol followed by 2× volumes of chloroform and mixed vigorously. The phases were separated by centrifugation, the bottom organic layer was removed, and the remaining aqueous layer was extracted again with 2× volumes of chloroform. The organic layers were pooled, dried under nitrogen, and reconstituted in potassium phosphate (0.2 M, pH 7.8). Samples (10 μL) were loaded onto a Phenomenex Luna C18(2) column (2.0 × 250 mm, 5 μm, Torrence, CA) equilibrated with 90% solvent A (0.5% formic acid in H_2O) and 10% solvent B (0.5% formic acid in MeOH) at a flow rate of 0.3 mL/min. The solvent was programmed as follows: a linear gradient from equilibration conditions to 20% B in 10 min, holding at 20% B for 10 min, increasing to 80% B in 0.1 min, holding for 5 min, decreasing to 10% B in 0.1 min, and re-equilibrating to initial conditions. Eluting compounds were detected by liquid chromatography/mass spectrometry (LC/MS). Positive ion electrospray ionization was employed with the following parameters: spray voltage = 4.0 kV; capillary temperature = 325 °C; sheath gas = 52 psi; tube lens offset = 46 V; auxiliary gas = 56. Samples were analyzed by selected-ion monitoring.

Liver Cytosol Incubations. All sample preparations were performed at 4 °C. The final incubation conditions for the kinetic determinations contained 5 mg/mL RLC, varied concentrations of either M_1G (0.5, 10, 25, 50, 100, 150, 200, and 250 μM) or 6-oxo-M_1G (5, 20, 40, 60, 80, 100, 150, 200, 400, 600, and 900 μM) and 0.4% DMSO in 0.2 M potassium phosphate (pH 7.8). IC_{50} determinations were carried out in 0.2 M potassium phosphate (pH 7.8) and 5 mg/mL RLC at the calculated K_m for each substrate (M_1G = 105 μM and 6-oxo-M_1G = 210 μM). The inhibitors were diluted in DMSO (0.4% total reaction volume). Reagents were equilibrated to 37 °C for 5 min and the reaction initiated by the addition of the substrate. Reactions were terminated after 60 min by adding two volumes of ice-cold ethanol, vortexed, and extracted twice with two volumes of chloroform. The extracts were evaporated under nitrogen, reconstituted in H_2O, and analyzed by HPLC-UV. The extraction of M_1G from RLC into ethanol/chloroform resulted in a 60 to 70% recovery from RLC incubations. Samples were separated on a Phenomenex Luna C18(2) column (4.6 × 250 nm, 5 μm) equilibrated with 90% solvent A (0.5% formic acid in H_2O) and 10% solvent B (0.5% formic acid in MeOH) at a flow rate of 1.0 mL/min. The solvent was programmed as follows: a linear gradient from the equilibration conditions to 20% B in 10 min, holding at 20% B for 10 min, increasing to 80% B in 0.1 min, holding for 5 min, decreasing to 10% B in 0.1 min, and re-equilibrating to initial conditions. Samples from the kinetic determinations were quantified in reference to a standard curve prepared by spiking known concentrations of either M_1G (0.5. 25, 50, 100, 200, and 300 μM) or 6-oxo-M_1G (5, 50, 100, 300, 500, 700, and 900 μM) into 5 mg/mL RLC solutions, followed immediately by termination, extraction, and analysis as outlined above. The extraction of 6-oxo-M_1G from RLC into ethanol/chloroform resulted in a 40 to 50% recovery from RLC incubations. All incubations and standards were performed in triplicate. The IC_{50} values were calculated on the basis of the inhibition of substrate consumption (of M_1G) or product production (of 2,6-dioxo-M_1G) in reference to the vehicle (DMSO) control. v_{max}/K_m and IC_{50} values were calculated with Prism software (Version 4.0c) using nonlinear regression one-site binding and one-site competition models, respectively.

Biochemical Synthesis of M_1G Metabolites. M_1G was incubated at 250 μM in purified bovine XO (0.1 U) and allowed to react for 60 min. Incubations were pooled in a separatory funnel and mixed with 100 mL of ethanol, followed by 100 mL chloroform, and shaken vigorously. The bottom organic layer was removed, and the extraction was repeated a second time. The organic layers were pooled, dried with magnesium sulfate, and evaporated to dryness. The remaining residue was dissolved in HPLC-grade H_2O and purified by semipreparative HPLC on a Phenomenex Luna C18(2) column (10 × 250, 10 μm). Isocratic elution (5 mL/min, 95:5 (H_2O/MeOH), containing 0.5% formic acid) provided the baseline resolution for eluting peaks: M_1G (∼20 min), 6-oxo-M_1G (∼24 min), and 2,6-dioxo-M_1G (∼30 min). Each peak was collected, pooled, and extracted as above (twice with 2× volume ethanol/chloroform, pooled, dried, and evaporated). The remaining product was attached to a vacuum pump to remove the residual formic acid carried over from the HPLC mobile phase. Samples were dissolved in d_6-DMSO and analyzed on a 400 MHz NMR.

1. Pyrimido[1,2-*f*]purin-6,10(3*H*,5*H*)-dione (6-oxo-M_1G). ^{1}H NMR (400 MHz, d_6-DMSO): δ 8.64 (d, 1H, J = 8 Hz, H_8), 8.06 (s, 1H, H_2), 6.21 (m, 1H, J = 8 Hz, H_7). ESI-MS *m/z*: 204.3.

2. Pyrimido[1,2-*f*]purin-2,6,10(1*H*,3*H*,5*H*)-trione (2,6-dioxo-M_1G). ^{1}H NMR (400 MHz, d_6-DMSO): δ 10.73 (s, 2.5H, N_1/N_3-H), 8.56 (d, 1H, J = 8 Hz, H_8), 6.18 (m, 1H, J = 8 Hz, H_7). ^{1}H NMR (400 MHz, d_6-DMSO with D_2O): δ 8.57 (d, 1H, J = 8 Hz, H_7), 6.20 (m, 1H, J = 8 Hz, H_7). ESI-MS *m/z*: 220.3.

3. Chemical Synthesis of Pyrimido[1,2-*f*]purin-6,10(3*H*,5*H*)-dione (6-oxo-M_1G). 6-Oxo-M_1dG synthesis was carried out as

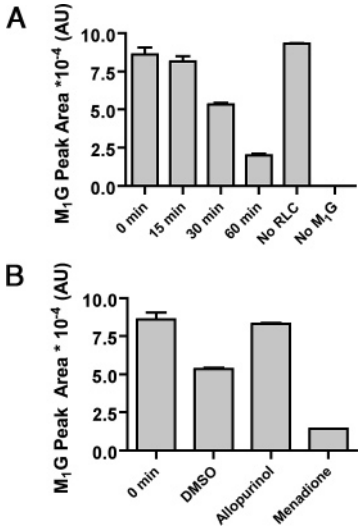

Figure 1. Time course of M_1G consumption in RLC and the effect of allopurinol and menadione on M_1G metabolism. All samples were incubated at 37 °C with 5 mg/mL RLC and 50 μM M_1G. (A) Time-dependent decrease in M_1G peak area following incubation in RLC. (B) Effect of the vehicle (DMSO), allopurinol, and menadione on M_1G consumption after 30 min of incubation in RLC.

described with minor modifications (*32*). The resulting product, 6-oxo-M_1dG, was purified by reversed phase chromatography on a C-18 Biotage cartridge (25+S). The pooled fractions were subjected to acid hydrolysis (0.1 N HCl for 60 min) and re-purified on a C-18 Biotage cartridge. The resulting product was analyzed by LC-MS and NMR spectroscopy to confirm the structure. ^{1}H NMR (400 MHz, d_6-DMSO): δ 8.62 (d, 1H, J = 8 Hz, H_8), 8.04 (s, 1H, H_2), 6.18 (d, 1H, J = 8 Hz, H_7). ESI-MS *m/z*: 204.3.

Results

Metabolism of M_1G in Rat Liver Cytosol. On the basis of our previous studies with M_1dG, we began our investigation of M_1G metabolism with liver cytosol. We hypothesized that M_1G would undergo metabolism in a manner qualitatively similar to that of M_1dG and that XO and AO would be involved in the metabolism. To test these hypotheses, we performed incubations in the presence of characteristic inhibitors of XO and AO (allopurinol and menadione, respectively). Chemically synthesized M_1G was incubated at 50 μM in RLC (5 mg/mL) for various times (0, 15, 30, and 60 min). Allopurinol and menadione (160 μM) were also added to selected reactions and stopped after 30 min. The metabolism of M_1G was monitored by reversed phase HPLC coupled to UV detection, which allowed for the separation and detection of incubation products. This analysis demonstrated a time-dependent decrease in M_1G peak area (Figure 1A) throughout the duration of the incubation. The HPLC product profile revealed the appearance of a single metabolite (M_1G-M1) following 15 min of incubation. Further analysis revealed the appearance of a second metabolite (M_1G-M2) after 30 min of incubation and continued production of both metabolites at 60 min. Allopurinol co-incubation resulted in the total inhibition of metabolism, whereas the menadione-containing sample exhibited an increase in total metabolism (Figure 1B), as seen for M_1dG (*32*) and other XO substrates (*35*, *36*). The HPLC-UV traces did not reveal any additional peaks associated with M_1G metabolism in the presence or absence of inhibitors. Subsequent analysis of the incubation mixtures by LC-MS revealed the successive additions of 16 amu to M_1G, which resulted in the following increases: M_1G (MH^+ = 188.3) → M_1G-M1 (MH^+ = 204.3) → M_1G-M2 (MH^+ = 220.3) (Figure 3A).

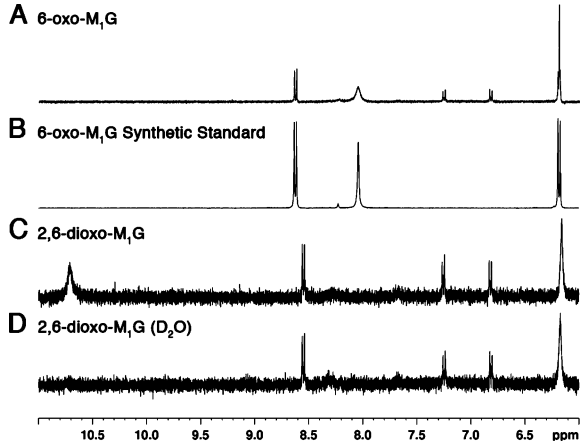

Figure 2. ^{1}H NMR of M_1G metabolites derived from biochemical or chemical synthesis. All samples were analyzed on a 400 MHz NMR in d_6-DMSO. (A) 6-oxo-M_1G was biochemically synthesized with bovine XO and (B) generated through chemical sythesis. (C) 2,6-Dioxo-M_1G was biochemically synthesized with bovine XO. (D) The addition of D_2O to the 2,6-dioxo-M_1G sample resulted in the loss of the chemical shift at 10.73 ppm, indicating an exchangeable proton.

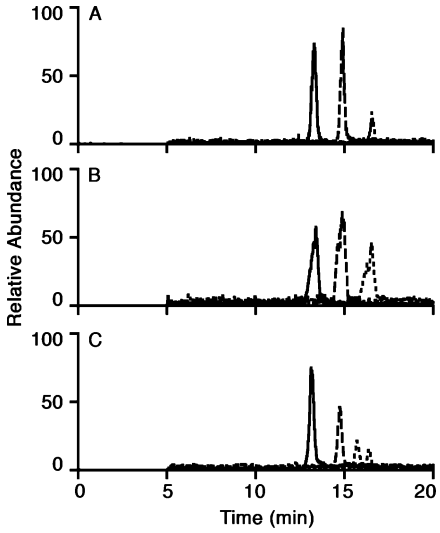

Figure 3. LC/MS chromatograms from the in vitro and in vivo metabolism of M_1G. Samples were analyzed by selected-ion monitoring of MH^+ = 188.3 (—), 204.3 (---), and 220.3 (···). LC/MS profiling of in vitro incubations with RLC (A) and bovine XO (B) revealed the successive additions of 16 amu to the parent ion M_1G (MH^+ = 188.3). (C) LC/MS analysis of urine collected from male Sprague Dawley rats that received iv M_1G (5 mg/kg).

Identification of M_1G Metabolites. As suggested by our in vitro observations in RLC, M_1G was investigated for its ability to undergo metabolism in incubations containing purified bovine XO. M_1G was rapidly oxidized by purified XO, producing both M_1G-M1 and M_1G-M2 (Figure 3B); therefore, purified bovine XO served as a platform to generate the metabolites for purification. The reaction was scaled up to 50 mL of total reaction volume and divided into separate 5 mL incubations. M_1G was incubated at a concentration of 250 μM and allowed to react for 60 min. Incubations were pooled, extracted, purified by semipreparative HPLC, and analyzed on a 400 MHz NMR.

Preliminary ^{1}H NMR analysis of M_1G-M1 (MH^+ = 204.3) revealed a spectrum (Figure 2A) rather similar to the previously characterized 6-oxo-M_1dG. The appearance of correlated peaks at 8.64 ppm (doublet) and 6.21 ppm (multiplet) suggested oxidation on the pyrimido ring because the singlet assigned as H_2 (8.06 ppm) remained in the spectrum. Further NMR studies by heteronuclear multiple bond correlation (HMBC) analysis

clearly revealed three-bond couplings of the proton assigned as H_8 to C_{4a}, C_6, and C_{10}. To verify the assignment of this structure, an authentic standard of 6-oxo-M_1G was synthesized. The synthetic standard displayed spectral properties identical to those of M_1G-M1 (Figure 2B). Together, these data confirmed the structure of M_1G-M1 as 6-oxo-M_1G.

The peaks appearing at 7.27 and 6.84 ppm in the biochemically purified 6-oxo-M_1G spectrum were determined to arise from impurities in the sample. This was confirmed by HMBC and saturation transfer experiments (Supporting Information Figures 1S and 2S, respectively). The HMBC revealed no three-bond couplings of these peaks to corresponding nuclei in the carbon spectrum, whereas the saturation transfer experiment determined that these peaks did not arise from a chemical equilibrium (i.e., equilibrium between the amide and imin-ol about C_6 and N_5 on the pyrimido ring). Furthermore, no trace of these peaks was observed in the authentic standard of 6-oxo-M_1G. Therefore, the peaks at 7.27 and 6.84 ppm were reasoned to be impurities derived from the purification process. The observed singlet at 6.21 ppm also appeared to be an impurity overlapping the signal from the H_7 doublet. However, its designation was not identified completely because of the overlap (this was also observed with the M_1G-M2 sample; see below).

^{1}H NMR analysis of M_1G-M2 ($MH^+ = 220.3$) identified correlated peaks at 8.56 ppm (doublet) and 6.18 ppm (singlet), suggesting that the C_7 and C_8 protons remained on the pyrimido ring. Notably, the singlet at 8.06 ppm from the 6-oxo-M_1G spectrum was not present in the M_1G-M2 sample, and a new singlet arose downfield at 10.73 ppm (Figure 2C). The appearance of the downfield peak and the disappearance of the singlet at 8.06 ppm are consistent with oxidation at C_2. The addition of D_2O to the sample resulted in the disappearance of the peak at 10.73 ppm, suggesting that this is an exchangeable proton (Figure 2D). Oxidation at C_2 on the imidazole ring of 6-oxo-M_1G is similar to oxidation at C_8 on 2′-deoxyguanosine (dG) in the formation of 8-oxo-dG. 8-Oxo-dG was used as a reference when assigning the positions of oxidation on M_1G. The oxidation of dG at C_8 lead to the appearance of a downfield peak at 10.75 ppm (in d_6-DMSO) attributed to the N_7-proton (*37*). Therefore, the chemical shift of 10.73 ppm was assigned to N_1/N_3-H's and the structure of M_1G-M2 was assigned as 2,6-dioxo-M_1G.

Peak impurities were also found in the 2,6-dioxo-M_1G spectrum. Most notable was the appearance of the singlet at 6.18 ppm, which also appeared in the spectrum of the biochemically synthesized 6-oxo-M_1G. In the 2,6-dioxo-M_1G spectrum, the singlet was likely overlapping with the doublet attributed to the H_7 proton at 6.18 ppm, which was inferred from the correlation seen in the 2D ^{1}H NMR analysis. The amount of material in the 2,6-dioxo-M_1G was low, and some impurity signals were evident.

Administration in Vivo of M_1G to Male Sprague Dawley Rats. To determine whether the enzymatic oxidations could occur in vivo, male Sprague Dawley rats were dosed intravenously with 5 mg/kg M_1G. The animals ($n = 3$) were housed in metabolic cages to collect urine and feces over the course of the experiment. Urine samples were extracted, chromatographed on a reversed phase column, and analyzed by LC-MS using selected ion monitoring. The parent compound (M_1G, $MH^+ = 188.3$) and the metabolites 6-oxo-M_1G ($MH^+ = 204.3$) and 2,6-dioxo-M_1G ($MH^+ = 220.3$) were monitored on separate channels of the same run. Analysis of the in vivo urine samples revealed molecular ions corresponding to M_1G (7.9 min), 6-oxo-M_1G (8.9 min), and 2,6-dioxo-M_1G (9.9 min). The molecular ions displayed retention times identical to those of the in vitro-generated metabolites from XO and RLC incubations (Figure 3) and the authentic standards for M_1G and 6-oxo-M_1G. The in vivo samples contained a background peak with a molecular ion of 220.3 (*m/z*) that eluted at 9.4 min. This peak also appeared in pre-dose and late time-point urine samples and did not correlate with 2,6-dioxo-M_1G production.

Scheme 2. Sequential Metabolism of M_1G to 6-Oxo-M_1G and 2,6-Dioxo-M_1G

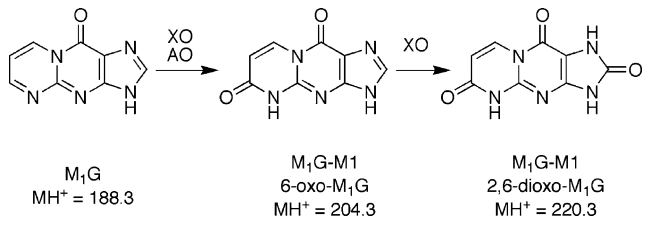

Kinetic Determinations in RLC with M_1G and 6-Oxo-M_1G. Following the characterization of the M_1G metabolites (Scheme 2), an investigation into their rates of formation was undertaken in vitro with RLC. Our preliminary data suggested that M_1G consumption in RLC led to the production of 6-oxo-M_1G, which then underwent an additional oxidation to 2,6-dioxo-M_1G. On the basis of inhibition experiments, XO appeared to be involved in the metabolism.

M_1G consumption was dependent on protein concentration and time of incubation in RLC. At 5 mg/mL RLC, M_1G consumption was linear out to 60 min of incubation. The kinetic determinations were performed by incubating M_1G at various concentrations for 60 min in the presence of 5 mg/mL RLC. The resulting products were extracted, separated by reversed phase chromatography, and analyzed by UV absorbance. M_1G consumption was quantified by reference to a standard curve that was prepared by spiking known concentrations of M_1G into RLC and terminating the reaction at time zero. This was followed by extraction and analysis identical to those for the incubated samples.

Figure 4A shows the velocity versus substrate concentration (v vs [S]) plot for the consumption of M_1G. The K_m was calculated to be 105 μM and the v_{max} at 126 pmol min^{-1} mg^{-1}. The total peak area of metabolites (both 6-oxo-M_1G and 2,6-dioxo-M_1G peak areas) versus [S] was also plotted (Figure 4B) to determine a K_m of 118 μM, which was in good agreement with that for substrate consumption. A plot of the peak areas for each metabolite versus [S] (Figure 4C) revealed that as the M_1G concentration increased, the ratio of 2,6-dioxo-M_1G to 6-oxo-M_1G decreased. This suggested that M_1G is capable of out-competing 6-oxo-M_1G at concentrations at or above its K_m in RLC.

Because the exact concentration of the enzyme(s) in the RLC was unknown, the relative catalytic efficiency for turnover was calculated by dividing the v_{max} by the K_m and normalizing the total protein concentration. Performing this analysis on the above data yielded a v_{max}/K_m of 0.005 min^{-1} mg^{-1} for M_1G consumption in RLC. An additional v versus [S] determination of M_1G consumption was also performed in a separate preparation of RLC, which yielded a K_m of 79 μM, a v_{max} of 84 pmol min^{-1} mg^{-1}, and a v_{max}/K_m of 0.004 min^{-1} mg^{-1}. The relative catalytic efficiencies of the turnover were in good agreement, whereas the K_m and v_{max} were not. This likely reflects the differences in makeup between the two separate preparations of RLC. Therefore, one may infer that the relative amounts of XO and AO (and any other enzyme that may be involved) in each

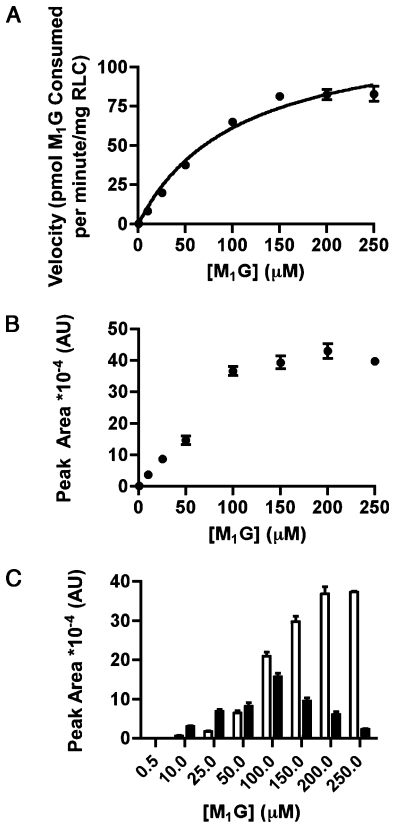

Figure 4. Kinetic determinations for M_1G consumption in RLC. (A) M_1G was incubated in RLC (5 mg/mL at 37 °C for 60 min) and quantified by reference to a standard curve. The data were analyzed by nonlinear regression and fit to a one site binding model: $K_m = 105$ μM and $v_{max} = 126$ pmol min^{-1} mg^{-1} ($v_{max}/K_m = 0.005$ min^{-1} mg^{-1}). (B) Plot of the total metabolite peak area (both 6-oxo-M_1G and 2,6-dioxo-M_1G) vs [S] ($K_m = 118$ μM). (C) Plot of peak areas vs [M_1G] for 6-oxo-M_1G (□) and 2,6-dioxo-M_1G (■).

preparation vary to a degree, resulting in altered kinetic parameters.

Kinetic determinations also were performed on the transformation of 6-oxo-M_1G to 2,6-dioxo-M_1G in RLC. Synthetic 6-oxo-M_1G was synthesized and used in the v versus [S] determinations. The incubations and analyses were performed as described for M_1G. On the basis of substrate consumption, a K_m for 6-oxo-M_1G was calculated at 210 μM and a v_{max} at 257 pmol min^{-1} mg^{-1}. The v_{max}/K_m was 0.005 min^{-1} mg^{-1}, which was the same value calculated for M_1G consumption in RLC. Therefore, it appears that both substrates are equally efficient in their turnover; however, M_1G possesses a higher apparent affinity (lower K_m) for the active site(s). This would allow M_1G to out-compete 6-oxo-M_1G at concentrations at or above the K_m for M_1G consumption, which was observed in the product profile from the M_1G kinetic determinations.

IC_{50} Determinations with Allopurinol in RLC. IC_{50} determinations were performed using various concentrations of allopurinol in RLC in the presence of M_1G and 6-oxo-M_1G. All substrates were incubated at their predetermined K_m. The percent inhibition was measured by the inhibition of substrate consumption or product production. These studies attempted to demonstrate the involvement of XO and AO in the metabolism of M_1G and 6-oxo-M_1G. An IC_{50} determination was first carried out with allopurinol using M_1G as a substrate. The amount of M_1G consumption at each concentration of allopurinol was determined on the basis of the peak area absorbance of M_1G and referenced to the vehicle control (no allopurinol) for percent consumption. On the basis of the inhibition of substrate

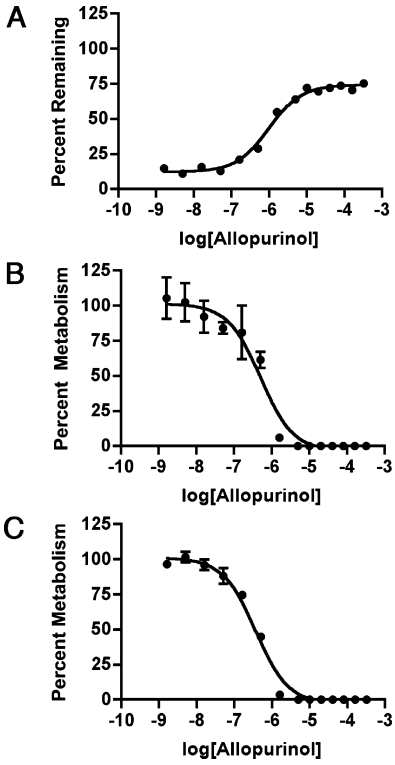

Figure 5. IC_{50} determinations in RLC with allopurinol using M_1G and 6-oxo-M_1G as substrates. (A) Using M_1G as a substrate, IC_{50} values were determined on the basis of substrate (M_1G) consumption (960 nM) and (B) inhibition of 2,6-dioxo-M_1G production (500 nM). (C) Using 6-oxo-M_1G as a substrate, the IC_{50} value was determined on the basis of the inhibition of 2,6-dioxo-M_1G production (360 nM).

consumption, an IC_{50} of 960 nM was determined (Figure 5A). At saturating concentrations of allopurinol (>20 μM), 25% of the M_1G was still consumed. This implied that an additional enzyme other than XO metabolized M_1G (presumably AO). An analysis of the product profile revealed two findings. First, no correlation existed between 6-oxo-M_1G production and allopurinol concentration (i.e., IC_{50} determination based on the inhibition of 6-oxo-M_1G production could not be determined). Second, at saturating concentrations of allopurinol (>20 μM), there was incomplete inhibition of 6-oxo-M_1G and total inhibition of 2,6-dioxo-M_1G production ($IC_{50} = 500$ nM). Together, these data suggested that XO catalyzed the conversion of M_1G to both 6-oxo-M_1G and 2,6-dioxo-M_1G, whereas the remaining enzyme activity, presumably that of AO, only converted M_1G to 6-oxo-M_1G.

Following these results, the IC_{50} was then determined with allopurinol using 6-oxo-M_1G as a substrate. The amount of 2,6-dioxo-M_1G produced at each concentration of allopurinol was determined on the basis of peak area absorbance and referenced to the vehicle control (no allopurinol) for percent inhibition. This resulted in an IC_{50} determination of 360 nM. These data confirmed that at saturating concentrations of allopurinol (>10 μM), no 2,6-dioxo-M_1G was produced and further implied that XO and not AO was the enzyme that acted on 6-oxo-M_1G in vitro. In a separate set of experiments, we investigated the contribution of AO to the metabolism of M_1G in RLC. Samples were incubated in the presence of M_1G (105 μM) and a saturating concentration of allopurinol (40 μM). To these reactions, increasing concentrations of menadione were added to generate an IC_{50} curve. A dose-dependent decrease in M_1G metabolism was observed with increasing concentrations of menadione ($IC_{50} = 5$ μM), which resulted in the total inhibition

Scheme 3. Biological Processing of M_1dG

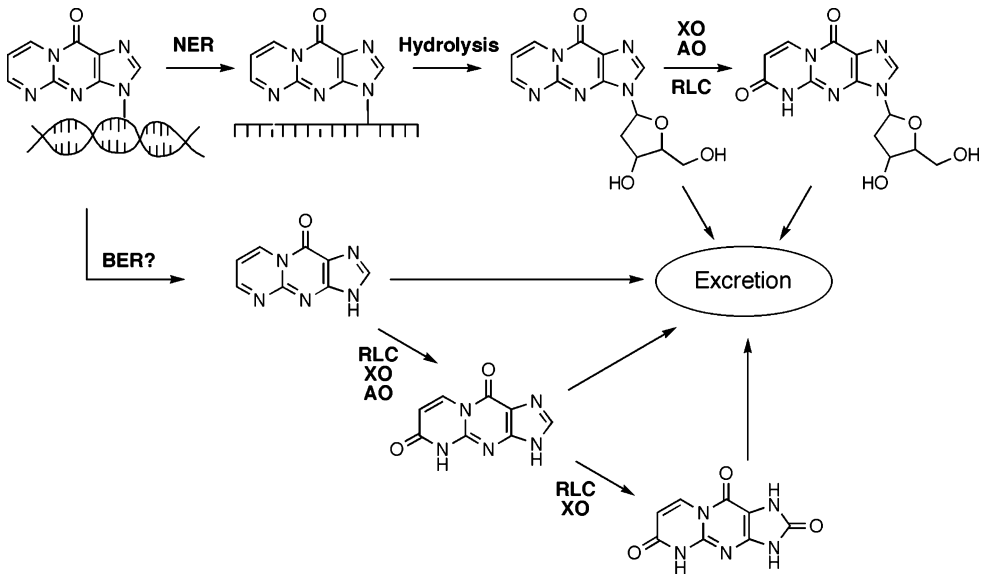

of the formation of both 6-oxo-M_1G and 2,6-dioxo-M_1G at saturating concentrations of menadione (>300 μM).

The IC_{50} with allopurinol was also calculated with M_1dG. The kinetic determinations for M_1dG conversion to 6-oxo-M_1-dG in RLC were determined previously (*32*). Upon the co-incubation of M_1dG (370 μM) with increasing concentrations of allopurinol, an IC_{50} of 120 nM was determined. It should be noted that at saturating concentrations of allopurinol (>5 μM), 6-oxo-M_1dG production was minimized but not completely inhibited. This suggests that AO is also contributing to the enzymatic oxidation of M_1dG in RLC.

Table 1. Kinetic and IC_{50} Determinations for M_1G, 6-Oxo-M_1G, and M_1dG in Rat Liver Cytosol

substrate	K_M (μM)	V_{max} (pmol min^{-1} mg^{-1})	V_{max}/K_M (min^{-1} mg^{-1})	IC_{50} (nM)
M_1G	105	126	0.005	960[a] 500[b]
6-oxo-M_1G	210	257	0.005	360
M_1dG	370[c]	104[c]	0.001	120

[a] The IC_{50} values were determined on the basis of the inhibition of M_1G consumption. [b] The IC_{50} values were determined on the basis of the inhibition of 2,6-dioxo-M_1G production with M_1G as a substrate. [c] The values are from Otteneder et al. (*32*).

Discussion

DNA adducts arise directly from, and downstream of, exposure to endogenously produced reactive oxygen species. In the absence of repair, these adducts may lead to mutations (point and frameshift), strand breaks, arrest in cell division, and induction of apoptosis. Successful repair of adducts leads to their removal from genomic DNA, thus averting these deleterious effects. Little is known about the fate of DNA adducts following their release from DNA. Our results suggest that the exposure of DNA adducts to endogenous oxidative enzymes results in the metabolism (oxidation) of the adducts. Oxidative metabolism of both deoxynucleoside-containing (*32*) and base adducts has now been observed.

The base adduct, M_1G, underwent sequential oxidative metabolism in vitro in RLC to two separate metabolites: 6-oxo-M_1G and 2,6-dioxo-M_1G. The production of each metabolite was also seen in vivo upon iv administration of M_1G to male Sprague Dawley rats. M_1G, 6-oxo-M_1G, and 2,6-dioxo-M_1G were all excreted in the urine, suggesting that these metabolites may be suitable for evaluation as urinary biomarkers under physiological conditions (Scheme 3). The kinetic parameters of M_1G and 6-oxo-M_1G metabolism were evaluated in RLC. These studies demonstrated that M_1G has a lower K_m than 6-oxo-M_1G in RLC, but each are metabolized with the same relative efficiency ($v_{max}/K_m = 0.005$ min^{-1} mg^{-1}). In comparison to M_1dG, both M_1G and 6-oxo-M_1G are better substrates (v_{max}/K_m for $M_1dG = 0.001$ min^{-1} mg^{-1}) and exhibited a lower K_m (Table 1).

M_1G, 6-oxo-M_1G, and M_1dG all appear to undergo oxidative metabolism by similar enzymes, namely, XO and AO. In RLC, approximately 75% of the M_1G metabolism (and all of the 6-oxo-M_1G metabolism) can be attributed to XO, as gauged by allopurinol inhibition. It should be noted that the relative amount of AO to XO activity in Sprague Dawley RLC is low. Other species, such as guinea pigs and rabbits, often contain higher ratios of AO to XO (*38*). Therefore, the total contribution of AO toward the metabolism of M_1G, 6-oxo-M_1G, and M_1dG may be underestimated in these studies.

The metabolism of each substrate is inhibited by co-incubation with allopurinol in RLC. Co-incubation of menadione, in the absence of allopurinol, resulted in the stimulation of metabolism for each substrate (*32*). This phenomenon of XO stimulation by menadione was first observed by Mahler et al. (*39*), continues to appear in the literature (*35*, *36*, *40*), and is seen in the metabolism of M_1dG (*32*). Stimulation by menadione was mitigated when saturating concentrations of allopurinol were used. Thus, this effect can be attributed to the stimulation of XO metabolism. When saturating concentrations of allopurinol were co-incubated with increasing concentrations of menadione, the ability of RLC to metabolize M_1G was abolished ($IC_{50} = 5$ μM).

Under physiological conditions, XO is believed to exist as a dehydrogenase (XD) (*41*). Manipulations ex vivo of the enzyme leads to irreversible proteolytic cleavage, or reversible oxidation (formation of disulfides), generating the oxidase form (*42*, *43*). Both forms of the enzyme are catalytically competent and capable of using molecular oxygen as a terminal electron acceptor, although XO is more efficient than XD at utilizing O_2 (*44*). XD can use NAD^+, which increases the efficiency of catalysis, and has no effect on XO (*44*). A preliminary evaluation of RLC did not reveal enhanced metabolism in the presence of

NAD^+, suggesting that the oxidase form is responsible for the oxidation of M_1dG, M_1G, and 6-oxo-M_1G in the liver cytosols evaluated.

The enzymatic conversion of M_1G to two separate oxidized metabolites is unique to the free base and not observed in metabolism studies with the deoxynucleoside, M_1dG. Furthermore, the sites of metabolism on M_1G are similar to the sites of oxidation on hypoxanthine, which is converted to xanthine, which is then oxidized to uric acid by XO/XD. Hypoxanthine oxidation occurs first at the 2-position on the pyrimidine ring (analogous to the 6-position on the pyrimido ring of M_1G) and subsequently on the 8-position of the imidazole ring (analogous to the 2-position on the imidazole ring of M_1G). Further metabolism of 6-oxo-M_1dG on the imidazole ring is likely prevented by the steric hindrance from the 2′-deoxyribose moiety.

When exogenously administered to male Sprague Dawley rats (5 mg/kg), M_1G was oxidized in vivo, and the principal metabolite (based on relative ionization) appeared to be 6-oxo-M_1G with 2,6-dioxo-M_1G being less abundant. These results were in agreement with the in vitro data, which suggested that at high concentrations, M_1G could out-compete 6-oxo-M_1G, thus minimizing the amount of 2,6-dioxo-M_1G produced. One may expect the ratio of 2,6-dioxo-M_1G to 6-oxo-M_1G to increase in vivo when lower concentrations of M_1G are present. However, the sensitivity at later time points during this analysis was too low to reliably address this hypothesis. When low concentrations of M_1G were incubated with RLC, a near complete conversion of M_1G to 2,6-dioxo-M_1G was observed (Figure 4C), which would suggest that upon physiological generation of M_1G in vivo, 2,6-dioxo-M_1G may be the main species observed.

The main route for repair of M_1dG residues in genomic DNA appears to be the NER pathway. Despite the fact that the BER and DNA glycosylase enzymes have never been definitively associated with M_1dG repair in vitro, one cannot rule out the involvement of these repair pathways in vivo. Considering the high degree of structural similarity between M_1dG and etheno adducts, it seems likely that a DNA glycosylase may catalyze the removal of M_1G from DNA.

The concept that repaired DNA adducts may undergo metabolism prior to urinary excretion has been previously investigated (*45*). Wang and Hecht evaluated the in vivo stability of the *N*-nitrosopyrrolidine (NPYR) guanine adduct, 2-amino-6,7,8,9-tetrahydro-9-hydroxypyrido[2,1-*f*]purin-4(3*H*)-one (N^7,C8-NPYR-Gua), by ip administeration of [^{14}C]-labeled N^7,C8-NPYR-Gua to male F-344 rats. The results from this study demonstrated that approximately 52% of the dose was recovered in the urine following 48 h of collection. HPLC with radioflow analysis revealed than 90% of the urinary radioactivity was recovered as the parent molecule (N^7,C8-NPYR-Gua), whereas the other 10% was distributed across several minor peaks, suggestive of metabolism. Neither the fate of the remaining 48% of the administered radioactivity nor the identity of the peaks in the urine profile was commented on by the investigators. It seems likely that N^7,C8-NPYR-Gua was eliminated in the feces and that N^7,C8-NPYR-Gua underwent significant excretion via the bile (as either the parent molecule or as a metabolite). These data demonstrate that exogenously administered adducts are subject to metabolism in vivo, with elimination, presumably, proceeding through multiple pathways.

These studies demonstrate that in addition to deoxynucleoside adducts, purine base adducts are subject to metabolism following repair in vivo (*32*, *45*). In the case of M_1G, the base is a better substrate for enzymatic oxidation than the deoxynucleoside (M_1-dG). Endogenous lesions are subject to multiple repair pathways. Following repair, these adducts are exposed to membrane-bound and cytosolic enzymes. Structural analogues of M_1G, M_1dG, and other exocyclic ring adducts are likely candidates to undergo metabolism in vitro and in vivo. Therefore, a yet undiscovered population of biomarkers may exist to assess exposure to oxidative damage in vivo.

Acknowledgment. We are grateful to the Mouse Metabolic Phenotyping Center for providing the rat metabolic cages used during these studies. We thank Celeste M. Riley and Stephen M. Doster for their careful reading of this manuscript. This work was supported by a research grant from the National Institutes of Health (CA87819). C.G.K. was supported by the United States Public Health Services grant T32 ES007028.

Supporting Information Available: ^{1}H NMR spectra obtained from the saturation transfer experiments and the heteronuclear multiple bond correlation experiments of the biochemically generated 6-oxo-M_1G. This information is available free of charge via the Internet at http://pubs.acs.org.

References

(1) Klaunig, J. E., and Kamendulis, L. M. (2004) The role of oxidative stress in carcinogenesis. *Annu. Rev. Pharmacol. Toxicol. 44*, 239−267.
(2) WHO (2001) *IPCS Environmental Health Criteria 222: Biomarkers and Risk Assessment: Validity and Validation*, World Health Organization, Geneva, Switzerland.
(3) Sharma, R. A., and Farmer, P. B. (2004) Biological relevance of adduct detection to the chemoprevention of cancer. *Clin. Cancer Res. 10*, 4901−4912.
(4) Chen, H. J., and Chang, C. M. (2004) Quantification of urinary excretion of 1,N^6-ethenoadenine, a potential biomarker of lipid peroxidation, in humans by stable isotope dilution liquid chromatography-electrospray ionization-tandem mass spectrometry: comparison with gas chromatography-mass spectrometry. *Chem. Res. Toxicol. 17*, 963−971.
(5) Jeong, Y. C., Sangaiah, R., Nakamura, J., Pachkowski, B. F., Ranasinghe, A., Gold, A., Ball, L. M., and Swenberg, J. A. (2005) Analysis of M_1G-dR in DNA by aldehyde reactive probe labeling and liquid chromatography tandem mass spectrometry. *Chem. Res. Toxicol. 18*, 51−60.
(6) Chen, H. J., and Chiu, W. L. (2005) Association between cigarette smoking and urinary excretion of 1,N^2-ethenoguanine measured by isotope dilution liquid chromatography-electrospray ionization/tandem mass spectrometry. *Chem. Res. Toxicol. 18*, 1593−1599.
(7) Zhang, S., Villalta, P. W., Wang, M., and Hecht, S. S. (2006) Analysis of crotonaldehyde- and acetaldehyde-derived 1,N^2-propanodeoxyguanosine adducts in DNA from human tissues using liquid chromatography electrospray ionization tandem mass spectrometry. *Chem. Res. Toxicol. 19*, 1386−1392.
(8) Dedon, P. C., Plastaras, J. P., Rouzer, C. A., and Marnett, L. J. (1998) Indirect mutagenesis by oxidative DNA damage: formation of the pyrimidopurinone adduct of deoxyguanosine by base propenal. *Proc. Natl. Acad. Sci. U.S.A. 95*, 11113−11116.
(9) Zhou, X., Taghizadeh, K., and Dedon, P. C. (2005) Chemical and biological evidence for base propenals as the major source of the endogenous M_1dG adduct in cellular DNA. *J. Biol. Chem. 280*, 25377−25382.
(10) Jeong, Y. C., and Swenberg, J. A. (2005) Formation of M_1G-dR from endogenous and exogenous ROS-inducing chemicals. *Free Radical Biol. Med. 39*, 1021−1029.
(11) Seto, H., Okuda, T., Takesue, T., and Ikemura, T. (1983) Reaction of malondialdehyde with nucleic acid. I. Formation of fluorescent pyrimido[1,2-a]purin-10(3H)-one nucleosides. *Bull. Chem. Soc. Jpn. 56*, 1799−1802.
(12) Basu, A. K., O'Hara, S. M., Valladier, P., Stone, K., Mols, O., and Marnett, L. J. (1988) Identification of adducts formed by reaction of guanine nucleosides with malondialdehyde and structurally related aldehydes. *Chem. Res. Toxicol. 1*, 53−59.
(13) Fink, S. P., Reddy, G. R., and Marnett, L. J. (1997) Mutagenicity in Escherichia coli of the major DNA adduct derived from the endogenous mutagen malondialdehyde. *Proc. Natl. Acad. Sci. U.S.A. 94*, 8652−8657.
(14) Basu, A. K., and Marnett, L. J. (1983) Unequivocal demonstration that malondialdehyde is a mutagen. *Carcinogenesis 4*, 331−333.

(15) Niedernhofer, L. J., Daniels, J. S., Rouzer, C. A., Greene, R. E., and Marnett, L. J. (2003) Malondialdehyde, a product of lipid peroxidation, is mutagenic in human cells. *J. Biol. Chem. 278*, 31426−31433.
(16) VanderVeen, L. A., Hashim, M. F., Shyr, Y., and Marnett, L. J. (2003) Induction of frameshift and base pair substitution mutations by the major DNA adduct of the endogenous carcinogen malondialdehyde. *Proc. Natl. Acad. Sci. U.S.A. 100*, 14247−14252.
(17) Sun, X., Nair, J., and Bartsch, H. (2004) A modified immuno-enriched ^{32}P-postlabeling method for analyzing the malondialdehyde-deoxyguanosine adduct, 3-(2-deoxy-β-D-erythro-pentofuranosyl)-pyrimido-[1,2-α]purin-10(3H)one in human tissue samples. *Chem. Res. Toxicol. 17*, 268−272.
(18) Kadiiska, M. B., Gladen, B. C., Baird, D. D., Germolec, D., Graham, L. B., Parker, C. E., Nyska, A., Wachsman, J. T., Ames, B. N., Basu, S., Brot, N., Fitzgerald, G. A., Floyd, R. A., George, M., Heinecke, J. W., Hatch, G. E., Hensley, K., Lawson, J. A., Marnett, L. J., Morrow, J. D., Murray, D. M., Plastaras, J., Roberts, L. J., 2nd, Rokach, J., Shigenaga, M. K., Sohal, R. S., Sun, J., Tice, R. R., Van Thiel, D. H., Wellner, D., Walter, P. B., Tomer, K. B., Mason, R. P., and Barrett, J. C. (2005) Biomarkers of oxidative stress study II: Are oxidation products of lipids, proteins, and DNA markers of CCl_4 poisoning? *Free Radical Biol. Med. 38*, 698−710.
(19) Jeong, Y. C., Nakamura, J., Upton, P. B., and Swenberg, J. A. (2005) Pyrimido[1,2-a]-purin-10(3H)-one, M_1G, is less prone to artifact than base oxidation. *Nucleic Acids Res. 33*, 6426−6434.
(20) Johnson, K. A., Fink, S. P., and Marnett, L. J. (1997) Repair of propanodeoxyguanosine by nucleotide excision repair in vivo and in vitro. *J. Biol. Chem. 272*, 11434−8.
(21) Hoberg, A. M., Otteneder, M., Marnett, L. J., and Poulsen, H. E. (2004) Measurement of the malondialdehyde-2′-deoxyguanosine adduct in human urine by immuno-extraction and liquid chromatography/atmospheric pressure chemical ionization tandem mass spectrometry. *J. Mass Spectrom. 39*, 38−42.
(22) Marnett, L. J., Riggins, J. N., and West, J. D. (2003) Endogenous generation of reactive oxidants and electrophiles and their reactions with DNA and protein. *J. Clin. Invest. 111*, 583−593.
(23) Reardon, J. T., Bessho, T., Kung, H. C., Bolton, P. H., and Sancar, A. (1997) In vitro repair of oxidative DNA damage by human nucleotide excision repair system: possible explanation for neurodegeneration in xeroderma pigmentosum patients. *Proc. Natl. Acad. Sci. U.S.A. 94*, 9463−9468.
(24) Hazra, T. K., Hill, J. W., Izumi, T., and Mitra, S. (2001) Multiple DNA glycosylases for repair of 8-oxoguanine and their potential in vivo functions. *Prog. Nucleic Acid Res. Mol. Biol. 68*, 193−205.
(25) Gallinari, P., and Jiricny, J. (1996) A new class of uracil-DNA glycosylases related to human thymine-DNA glycosylase. *Nature 383*, 735−738.
(26) Singer, B., Antoccia, A., Basu, A. K., Dosanjh, M. K., Fraenkel-Conrat, H., Gallagher, P. E., Kusmierek, J. T., Qiu, Z. H., and Rydberg, B. (1992) Both purified human 1,N^6-ethenoadenine-binding protein and purified human 3-methyladenine-DNA glycosylase act on 1,N^6-ethenoadenine and 3-methyladenine. *Proc. Natl. Acad. Sci. U.S.A. 89*, 9386−9390.
(27) Oesch, F., Adler, S., Rettelbach, R., and Doerjer, G. (1986) Repair of etheno DNA adducts by N-glycosylases. *IARC Sci. Publ.* 373−379.
(28) Saparbaev, M., and Laval, J. (1998) 3,N^4-ethenocytosine, a highly mutagenic adduct, is a primary substrate for Escherichia coli double-stranded uracil-DNA glycosylase and human mismatch-specific thymine-DNA glycosylase. *Proc. Natl. Acad. Sci. U.S.A. 95*, 8508−8513.
(29) Saparbaev, M., Kleibl, K., and Laval, J. (1995) Escherichia coli, Saccharomyces cerevisiae, rat and human 3-methyladenine DNA glycosylases repair 1,N^6-ethenoadenine when present in DNA. *Nucleic Acids Res. 23*, 3750−3755.
(30) Powell, C. L., Swenberg, J. A., and Rusyn, I. (2005) Expression of base excision DNA repair genes as a biomarker of oxidative DNA damage. *Cancer Lett. 229*, 1−11.
(31) Wood, R. D., Mitchell, M., Sgouros, J., and Lindahl, T. (2001) Human DNA repair genes. *Science 291*, 1284−1289.
(32) Otteneder, M. B., Knutson, C. G., Daniels, J. S., Hashim, M., Crews, B. C., Remmel, R. P., Wang, H., Rizzo, C., and Marnett, L. J. (2006) In vivo oxidative metabolism of a major peroxidation-derived DNA adduct, M_1dG. *Proc. Natl. Acad. Sci. U.S.A. 103*, 6665−6669.
(33) Schnetz-Boutaud, N. C., Mao, H., Stone, M. P., and Marnett, L. J. (2000) Synthesis of oligonucleotides containing the alkali-labile pyrimidopurinone adduct, M_1G. *Chem. Res. Toxicol. 13*, 90−95.
(34) Guengerich, F. P. (1994) Analysis and Characterization of Enzymes, in *Principles and Methods of Toxicology* (Hayes, A. W., Ed.) pp 1259−1313, Raven Press, Ltd., New York, NY.
(35) Obach, R. S. (2004) Potent inhibition of human liver aldehyde oxidase by raloxifene. *Drug Metab. Dispos. 32*, 89−97.
(36) Yoshihara, S., and Tatsumi, K. (1986) Kinetic and inhibition studies on reduction of diphenyl sulfoxide by guinea pig liver aldehyde oxidase. *Arch. Biochem. Biophys. 249*, 8−14.
(37) Cho, B. P., Kadlubar, F. F., Culp, S. J., and Evans, F. E. (1990) ^{15}N nuclear magnetic resonance studies on the tautomerism of 8-hydroxy-2′-deoxyguanosine, 8-hydroxyguanosine, and other C_8-substituted guanine nucleosides. *Chem. Res. Toxicol. 3*, 445−452.
(38) Beedham, C. (2002) Molybdenum Hydroxylases, in *Enzyme Systems That Metabolise Drugs and Other Xenobiotics* (Ioannides, C., Ed.) pp 147−187, John Wiley & Sons, Chichester, NY.
(39) Mahler, H. R., Fairhurst, A. S., and Mackler, B. (1955) Studies on metalloflavoproteins. IV. The role of the metal. *J. Am. Chem. Soc. 77*, 1514−1521.
(40) Rajagapolan, K. V., Fridovich, I., and Handler, P. (1962) Hepatic aldehyde oxidase: I. Purification and properties. *J. Biol. Chem. 237*, 922−928.
(41) Stirpe, F., and Della Corte, E. (1969) The regulation of rat liver xanthine oxidase. Conversion in vitro of the enzyme activity from dehydrogenase (type D) to oxidase (type O). *J. Biol. Chem. 244*, 3855−3863.
(42) Waud, W. R., and Rajagopalan, K. V. (1976) Purification and properties of the NAD+-dependent (type D) and O2-dependent (type O) forms of rat liver xanthine dehydrogenase. *Arch. Biochem. Biophys. 172*, 354−364.
(43) Della Corte, E., Gozzetti, G., Novello, F., and Stirpe, F. (1969) Properties of the xanthine oxidase from human liver. *Biochim. Biophys. Acta 191*, 164−166.
(44) Hunt, J., and Massey, V. (1992) Purification and properties of milk xanthine dehydrogenase. *J. Biol. Chem. 267*, 21479−21485.
(45) Wang, M., and Hecht, S. S. (1997) A cyclic N^7,C-8 guanine adduct of N-nitrosopyrrolidine (NPYR): formation in nucleic acids and excretion in the urine of NPYR-treated rats. *Chem. Res. Toxicol. 10*, 772−778.

TX600334X